Food Chemistry 138 (2013) 1856–1867

Contents lists available at SciVerse ScienceDirect

Food Chemistry

journal homepage: www.elsevier.com/locate/foodchem

Dung-shen (*Codonopsis pilosula*) attenuated the cardiac-impaired insulin-like growth factor II receptor pathway on myocardial cells

Kun-Hsi Tsai [a,b,c], Nien-Hung Lee [d], Guei-Ying Chen [e], Wei-Syun Hu [f], Chen-Yen Tsai [g], Mu-Hsin Chang [h], Gwo-Ping Jong [h], Chia-Hua Kuo [i], Bor-Show Tzang [j], Fuu-Jen Tsai [k], Chang-Hai Tsai [l], Chih-Yang Huang [d,k,m,*]

[a] *Department of Emergency, China Medical University Beigang Hospital, Yunlin County, Taiwan*
[b] *Department of Emergency Medicine, Chi Mei Medical Center, Liouying, Tainan, Taiwan*
[c] *Department of Biological Science and Technology, National Chiao Tung University, Hsinchu, Taiwan*
[d] *Graduate Institute of Basic Medical Science, China Medical University, Taichung, Taiwan*
[e] *Department of Gastroenterology, National Taiwan University Hospital, Taiwan*
[f] *Division of Cardiology, Taipei Medical University Shuang-Ho Hospital, Taipei, Taiwan*
[g] *Department of Pediatrics, China Medical University Beigang Hospital, Yunlin, Taiwan*
[h] *Division of Cardiology, Department of Internal Medicine, Armed Force Taichung General Hospital, Taichung, Taiwan*
[i] *Laboratory of Exercise Biochemistry, Taipei Physical Education College, Taipei, Taiwan*
[j] *Institute of Biochemistry and Biotechnology, Chung Shan Medical University, Taichung, Taiwan*
[k] *Graduate Institute of Chinese Medical Science, China Medical University, Taichung, Taiwan*
[l] *Department of Healthcare Administration, Asia University, Taichung, Taiwan*
[m] *Department of Health and Nutrition Biotechnology, Asia University, Taichung, Taiwan*

ARTICLE INFO

Article history:
Received 6 July 2011
Received in revised form 8 August 2012
Accepted 9 November 2012
Available online 20 November 2012

Keywords:
Angiotensin II
Apoptosis
Calcium influx
Codonopsis pilosula
Leucine[27]-insulin like growth factor II
Mitochondrial outer-membrane permeability

ABSTRACT

Previous studies from our lab showed that increase in AngII in H9c2 cells causes elevated IGFII and IGFIIR through MEK and JNK, leading to rise in intracellular calcium, calcineurin activation by PLC-β3 *via* Gαq, insertion into mitochondrial membranes of Bad, and apoptosis *via* caspases 9 and 3. *Codonopsis pilosula* is traditionally used to lower blood pressure. The purpose of our study is to investigate if *C. pilosula* attenuates AngII plus Leu[27]-IGFII-induced calcium influx and apoptosis in H9c2 cardiomyoblasts. *C. pilosula* significantly attenuated AngII induced IGFIIR promoter activity. Leu[27]-IGFII was applied to enhance the AngII effect. *C. pilosula* also reversed Ca^{2+} influx, MOMP and apoptosis increased by AngII plus Leu[27]-IGFII. Molecular markers in IGFIIR apoptotic pathway (IGFIIR, calcineurin, etc.) and IGFIIR-Gαq association were downregulated by *C. pilosula*. However, p-Bad[Ser136] and Bcl-2 were increased. Therefore, *C. pilosula* suppresses AngII plus Leu[27]-IGFII-induced IGFII/IGFIIR pathway in myocardial cells.

1. Introduction

Insulin growth factor I (IGFI) is a 70 amino acids long polypeptide hormone growth factor with molecular weight of 7649 Daltons that structurally resembles insulin. IGFI is produced in the liver under the control of pituitary growth hormone it binds to IGFI binding proteins (IGFBPs) to be carried to target tissues or cells by the circulatory system (Delafontaine, Song, & Li, 1995). Once it finds its target, IGFI binds to cell surface IGFI receptor (IGFIR) with a high specificity. IGFI gene is located on chromosome 12 in humans and chromosome 10 in mice.

IGFI receptor contains 2 extracellular α-chains and 2 intracellular β-chains (Delafontaine et al., 1995). IGFIR is a receptor tyrosine kinase, which dimerizes once IGFI is bound and whose intracellular domain becomes autophosphorylated (Tsuruzoe, Emkey, Kriauciunas, Ueki, & Kahn, 2001). The phosphorylated tyrosine residues can be found in Src homology 2 domains, which then activate insulin receptor substrate 1 and Shc by phosphorylation *via* growth factor receptor binding protein 2. Subsequently, phosphatidylinositol 3-kinase is activated, which then activates Akt. Finally, Akt phosphorylates at serine 136 on Bad and then unphosphorylated Bad departures from mitochondrial membranes, stabilizing mitochondrial membrane potential and inducing cell survival. In

* Corresponding author at: Graduate Institute of Basic Medical Science, Graduate Institute of Chinese Medical Science, China Medical University and Hospital, No. 91, Hsueh-Shih Road, Taichung 404, Taiwan. Tel.: +886 4 22053366x3313.
E-mail address: cyhuang@mail.cmu.edu.tw (C.-Y. Huang).

0308-8146/$ - see front matter © 2012 Elsevier Ltd. All rights reserved.
http://dx.doi.org/10.1016/j.foodchem.2012.11.056

addition, depending on the cell type, IGFI/IGFIR can lead to cell proliferation via Ras/Raf/MEK/ERK pathway or cell migration *via* Rac.

IGFI gene expression in rat liver declines with advancing age, and comes to its lowest levels in young adulthood (LeRoith, Werner, Beitner-Johnson, & Roberts, 1995). Other organs, such as brain and heart, also display different IGFI expression patterns in different developmental stages. These may be caused by different prepro-IGFIs. This also occurs in humans. In a human placental IGFI receptor model, IGFIR autoantibodies and therefore IGFI resistance were found in certain patients with diabetes or rheumatic disorders (Tappy, Fujita-Yamaguchi, LeBon, & Boden, 1988).

IGFII gene is located in chromosome 11p15, 30 kilo-bases long, and composed of 9 exons and 4 promoters. IGFII is an imprinted gene and associated with allele-specific CpG methylation patterns in IGFII-H19 region (Park & Buetow, 1991; Sklar et al., 1992). IGFII prepro-hormone (20.1 kilo-Daltons (kDa)) is cleaved to generate 7.5 kDa, 67-amino-acid-long IGFII monomer, which is 47% identical to insulin (Park & Buetow, 1991). IGFII is synthesised in the liver and binds to type I IGF receptor with higher affinity than that of type II, initiating a tyrosine kinase activity and a protein kinase cascade. Moreover, IGFII receptor (IGFIIR) functions as a clearance receptor and a possible IGFBP in foetus. Therefore, IGFII was categorised as an embryonic gene (O'Dell & Day, 1998).

IGFIIR, also called cation-independent mannose-6-phosphate receptor, is a protein that in humans is encoded by the IGFIIR gene (Humbel, 1990). IGFIIR is a multifunctional protein receptor that binds insulin-like growth factor II (IGFII) at the cell surface and mannose-6-phosphate (M6P)-tagged proteins in the trans-Golgi network (Oshima, Nolan, Kyle, Grubb, & Sly, 1988). IGFIIR is a type I transmembrane protein containing a large extracellular domain, a relatively short intracellular tail and a transmembrane domain (Laureys, Barton, Ullrich, & Francke, 1988). The extracellular domain consists of a small region homologous to the collagen-binding domain of fibronectin and 15 repeats of approximately 147 amino acids (AA) in length. Each of these repeats is homologous to the 157-residue extracellular domain of mannose 6-phosphate receptor. IGFII binding is mediated through one of the repeats, while two different repeats are responsible for binding to M6P. The IGFIIR is approximately 300 kDa in size it appears to exist and function as a dimer.

IGFII plays a role in mammalian postnatal and foetal growth functioning in an autocrine or paracrine manner. SHR rats display high levels of ventricular and heart IGFII and IGFIIR, and low levels of IGFI mRNA and protein expression during foetal, neonatal and postnatal periods (Engelmann, Boehm, Haskell, Khairallah, & Ilan, 1989; Ghosh, Dahms, & Kornfeld, 2003), whereas limb, muscle, lungs, intestine, kidneys, liver and brain vary in degree of low IGFIIR mRNA concentration (Brown et al., 1986). However, IGFII expression declines after birth and it goes through a transition during the neonatal stage (Engelmann et al., 1989). In a porcine model of brief coronary occlusions, which resulted in prolonged contractile dysfunctions and increased tolerance of myocardium against repeated challenges, such as ischaemia/reperfusion, expression of IGFII and IGFBP-5 were activated under stressful conditions (Kluge et al., 1995). In addition, Matthews etc. postulated that following myocardial infarction, high IGFII expressions were shown in cardiomyocytes in surviving and necrotic areas of post-infarct myocardium (Matthews et al., 1999). Therefore, IGFII seemed to act as a rescuer.

The IGFII gene is imprinted and loss of its imprinting or otherwise overexpression is involved in several growth disorders and tumors, including Beckwith–Wiedemann syndrome (BWS) (Sun, Dean, Kelsey, Allen, & Relk, 1997). BWS involves IGFII deregulation and is characterised by pre- and postnatal overgrowth, multiple organ overgrowth including macroglossia, and increased risk of developing childhood tumors. Similar phenomenon was observed in a mouse IGFII overexpression model, in which many BWS syndromes were displayed, such as prenatal overgrowth, polyhydramnios, foetal and neonatal lethality, disproportionate organ including heart and kidneys and skeletal abnormalities (Sun et al., 1997). Therefore, IGFII may be likely to cause damage rather than to protect.

The role of IGFII in cardiac hypertrophy has been debated for years. In 2002, IGFII was proved to induce hypertrophy in cultured adult cardiomyocytes *via* two alternative signalling pathways: an IGFI-dependent pathway *via* ERK1/2 or a lysosome-dependent pathway (Huang, Hao, & Buetow, 2002). IGFII expression can be induced under stressful conditions, such as brief coronary occlusions, in adult animals, as shown in a porcine model (Kluge et al., 1995).

The synthesis of angiotensin II (AngII) is a result of renin–angiotensin aldosterone system, which is a hormone cascade that maintains homeostases of arterial pressure, tissue perfusion, and extracellular volume (Atlas, 2007). The precursor of AngII, angiotensinogen (452 AAs long in human), is first synthesised in the liver and travel to the kidneys through blood stream to be converted to angiotensin I (AngI) (10 AAs long) by removal of N-terminal of the precursor by renin (Basso & Terragno, 2001), which is secreted by juxtaglomerular cells that line the afferent arteriole of the renal glomerulus (Atlas, 2007). AngI is converted to AngII (7–9 AAs long) by angiotensin converting enzyme in the lungs. AngII affects the cardiovascular system by causing vasoconstriction, increased blood pressure, increased cardiac contractility and vascular and cardiac hypertrophy (Atlas, 2007). In addition, AngII stimulates zona glomerulosa to secrete aldosterone to enhance re-absorption of Na^+ ions and water in distal tubules and collecting ducts and to promote K^+ secretion by binding to type I angiotensin receptor and *via* $G\alpha q$ (Atlas, 2007).

From previous studies of Dr. Chun-Hsien Chu and other senior graduates from our lab, AngII stimulated expression of IGFII and IGFIIR in H9c2 cardiomyoblasts, which are not terminally differentiated and displays properties of cardiomyocytes, via MEK and JNK (Lee et al., 2006). Then IGFIIR somehow activates calcineurin, which was previously known as phosphatase 2B, dephosphorylates Bad at serine 136. Un-phosphorylated Bad then inserts itself into mitochondrial membranes, causing mitochondrial outer-membrane permeability (MOMP) or mitochondrial membrane potential instability and release of mitochondrial proteins, such as Apaf-1 and cytochrome *c* (Cyto *c*). Apaf-1 and cytochrome *c* then form an apoptosome with pro-caspase 9, which is then converted to caspase 9. Finally, caspase 9 activates caspase 3, leading to apoptosis. This pathway was confirmed by using a mouse abdominal aortic ligation (which simulated pressure overload and induced AngII), IGFII antisense RNA, IGFIIR antibody, U-0126 (ERK inhibitor), SP-600125 (JNK inhibitor) and CsA (cyclosporine A; calcineurin inhibitor). Dr. Chu later proved that binding of IGFII to cell at serine 537 via $G\alpha q$ (Kuo et al., 2006). PLC-β3 cleaves phosphatidylinositol-4, 5-bisphosphate is cleaved into diacyl glycerol (DAG) and inositol 1, 4, 5-trisphosphate (IP_3). DAG remains bound to cell membrane, and IP_3 is released as a soluble structure into the cytosol (Heineke & Molkentin, 2006). IP_3 then diffuses through the cytosol to bind to IP_3 receptors, which are part of calcium channels in sarcoplasmic reticulum membrane. This causes an increase of cytosolic Ca^{2+} concentration, which activates calcineurin. Moreover, calcium and DAG together work to activate protein kinase Cα, which goes onto phosphorylate Na^+/Ca^{2+} exchanger in cell membrane of a cardiomyocyte, leading to a further increase in intracellular Ca^{2+} and calcineurin activity (Heineke & Molkentin, 2006). Calcineurin then dephosphorylates Bad for its insertion into mitochondrial membranes to cause MOMP, release of Apaf-1 and Cyto c, activation of caspases 9 and 3 and apoptosis.

Therefore, it was necessary to screen traditional Chinese medicine (TCM) herb to find out which one that suppresses

IGF-II-induced cardiomyocyte apoptosis. Dr. Chu previously cloned full-length and different truncated versions of IGFIIR promoter sequences (designated P1–P6) and ligated these DNA sequences to luciferase reporter gene in order to monitor IGFIIR promoter activity under treatment of AngII and TCMs. In this screening system, (negative control), CMV (positive control), P1 (full-length IGF-IIR promoter sequence) and PGL_2 plasmids was used. So far 61 TCMs were already tested and categorised according to their effective doses. Dung-shen (*Codonopsis pilosula*) was one of the TCMs that significantly reduced IGFIIR promoter activity at 1, 5, and 50 unit/μl (Fig. 1), and was selected for subsequent experiments.

Leu^{27}-IGFII is a 7.42 kDa, human IGFII analogue that is resulted from $tyrosine^{27}$-to-$leucine^{27}$ mutation (Sakano et al., 1991). Its affinity for IGFIIR in L6 myoblasts is about 16 nm. Leu^{27}-IGFII specifically binds to IGFIIR with a high affinity and is able to induce IGFIIR-induced H9c2 cell apoptosis via Gαq, which involves increased activity of PLC-β3, calcineurin, Bad, and caspases 9 and 3 (Chu et al., 2008).

Finally, *C. pilosula* is a perennial species of flowering plant native to Northeast Asia and Korea and usually found growing around stream banks and forest openings under the shade of trees. *C. pilosula* roots are used in traditional Chinese medicine to lower blood pressure, increase red and white blood cell numbers, cure appetite loss, strengthen the immune system, and replenish chi (Wang, Ng, Yeung, & Xu, 1996). The roots are harvested from the plant during the third or fourth year of growth and dried prior to sale.

In this study, we investigated whether *C. pilosula* may attenuate synergistic calcium influx and apoptosis induced by AngII plus Leu^{27}-IGFII in H9c2 cardiomyoblast cells and rat neonatal primary cells. The current findings revealed that AngII was able to increase IGFIIR promoter activity, which was reduced by *C. pilosula*, and that AngII plus Leu^{27}-IGFII induced Ca^{2+} influx, MOMP and apoptosis, and *C. pilosula* reversed these situations. AngII plus Leu^{27}-IGFII also unregulated levels of IGFIIR, Gαq, p-PLC-β3, calcineurin, Bad, cytochrome *c* and caspases 9 and 3, and *C. pilosula* downregulated their protein levels and even activities. *C. pilosula* also increased level of $p\text{-}Bad^{Ser136}$ and Bcl-2. Therefore, *C. pilosula* is able to reduce IGFIIR promoter activity, IGFIIR signalling pathway, MOMP and apoptosis induced by IGFIIR signalling activation in H9c2 cells.

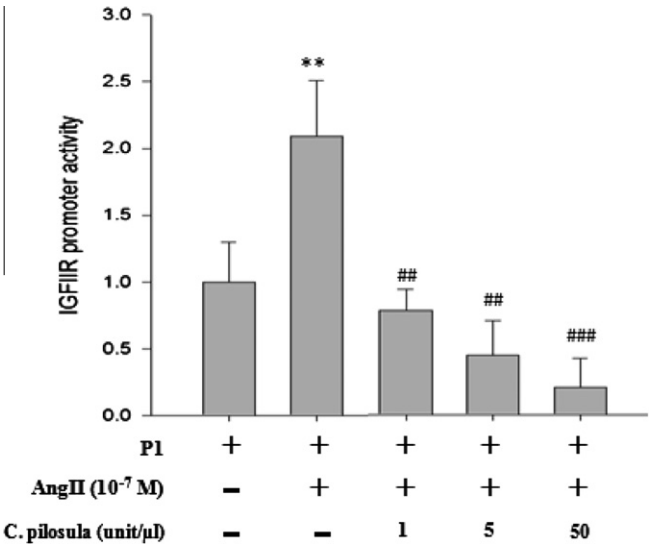

Fig. 1. IGFIIR promoter activity is induced by AngII and is reversed by *C. pilosula* Twenty-four hours after growing H9c2 cells in 24-well plates, P1 (full-length IGFIIR promoter) and PGL_2 plasmids were used for transfection after serum deprivation. *C. pilosula* was added 15 h after transfection, followed by AngII 1 h later. Luciferase assay was conducted 24 h after addition of AngII. $p < 0.01$ vs. P1, $^{\#\#}p < 0.01$ vs. P1 + AngII, and $^{\#\#\#}p < 0.001$ vs. P1 + AngII.

2. Materials and methods

2.1. Cell culture

H9c2 cardiomyoblast cells were purchased from American Type Culture Collection (ATCC; CRL-1446) (Rockville, MD, USA). The cells were cultured in Dulbecco's modified Eagle's medium (DMEM) (Sigma Aldrich, MO, USA) with 10% cosmic calf serum (CCS) (HyClone, USA) in humidified air with 5% CO_2 at 37 °C. Cell medium was changed 48 h after sub-cultivation. 5 ml Dulbecco's phosphate-buffered saline (PBS) (GIBCO, Auckland, New Zealand) was used to wash each culture plate or vessel. After the cells were deprived of serum (i.e. in serum-free DMEM) for 4 h and treated with different drugs at different concentrations and time points.

2.2. Neonatal rat primary cardiomyocytes culture

Neonatal Rat/Mouse Cardiomyocyte Isolation System Kit (Cellutron Life Technology, Baltimore, USA) was used to isolate and culture neonatal primary cardiomyocytes. 4 ml SureCoat solution (Cellutron Life Technology, Baltimore, USA) was used to coat each 10 cm plate for at least 1 h in humidified air with 5% CO_2 at 37 °C. Left ventricles from hearts of 1 to 2-day-old Sprague–Dawley (SD) rats were isolated and incubated in digestion solution at 37 °C. Each plate was coated by another 5 ml SureCoat at least 1 h in humidified air with 5% CO_2 at 37 °C. Then all isolated cells were placed on non-coating dishes for 1 h, heart fibroblasts attached to bottom of each plate and the floating cells were neonatal cardiomyocytes, which were then transferred to the pre-coated plates. Finally the cells were cultured in DMEM (10% CCS).

2.3. Luciferase assay

H9c2 cells were grown in 24-well plates containing DMEM (10% CCS) and incubated for 24 h in humidified air with 5% CO_2 at 37 °C. Plasmid–DMEM transfection mixtures containing Transfast™ transfection reagent (Promega, WI, USA) were prepared: CMV: PGL_2, Null: PGL_2 and P1: PGL_2. The plasmid–DMEM mixtures were added to appropriate wells. The cells were incubated for 1 h in humidified air (5% CO_2) at 37 °C and then additional DMEM (10% CCS) was added. The cells were incubated for 15 h in humidified air with 5% CO_2 at 37 °C. Different doses of *C. pilosula* (Ko-Da, Taiwan) solutions were added to appropriate wells. And then 10^{-7} M AngII (Angiotensin II human; AngII, Sigma, MO, USA) was added 1 h after administration of *C. pilosula*. Twenty-four hours after addition of AngII, 100 μl 1X passive lysis buffer (PLB, Promega, WI, USA) was added to each well to lyse cells. The 24-well plate was rocked for 15 min at room temperature and then vortexed for 30 s to avoid any precipitation in the bottom of each well. Luciferase Assay Substrate (Promega, WI, USA) was mixed with Luciferase Assay Buffer (Promega, WI, USA) (=LARII). 100 μl LARII per well was added. 20 μl samples from each well were transferred to a 96-well plate. Finally, luciferase activity was measured by MikroWin 2000 software (Berthold Technologies, Germany) and a nucleic acid quantification analyser (Mithras LB 940).

2.4. Fluo 4-AM staining assay

Fluo 4-AM ($C_{51}H_{50}F_2N_2O_{23}$, Invitrogen, Oregon, USA) is a Ca^{2+} chelator that binds to cytosolic Ca^{2+} and is able to absorb and emit light at 494 nm and 516 nm when Ca^{2+} is bound. Its K_d value for free Ca^{2+} is 345 nm. H9c2 cardiomyoblasts were grown in a 12-well plate (1×10^5 cells/well) containing DMEM (10% CCS). Twenty-four hours later, the cells were deprived of serum for 4 h, and then 20, 40, 60, 80 and 100 μg/ml *C. pilosula* were added to appropriate wells followed by 10 μl 10^{-7} M AngII 1 h later, followed by 10^{-8} M

Leu^{27}-IGFII after further 2 h. The cells were incubated in humidified air with 5% CO_2 at 37 °C. Twenty-four hours after administration of Leu^{27}-IGFII, 6 μl 1 mM Fluo 4-AM was added to each well in the absence of light and then the 12-well plate was placed in humidified air with 5% CO_2 at 37 °C for 30 min. Each well washed with 0.5 ml serum-free DMEM three times. Finally the cells were observed under fluorescent microscope with FITC.

2.5. Western blotting

H9c2 cells were grown in 10 cm culture dishes containing DMEM (10% CCS) to 80–90% confluency. Twenty-four hours later, the cells were deprived of serum for 4 h, and then 20, 40, and 60 μg/ml *C. pilosula* were added to appropriate dishes followed by 10^{-7} M AngII was added 1 h later, followed by 10^{-8} M Leu^{27}-IGFII after further 2 h. The cells were incubated in humidified air (5% CO_2) for 24 h at 37 °C. Twenty-four hours after administration of Leu^{27}-IGFII, each plate was washed with 3 ml PBS twice and the remaining fluid in each plate was sucked off. Then 100 μl cell lysis buffer (50 mM pH7.5 Tris-base, 0.5 M NaCl, 1 mM pH8 EDTA, 1 mM BME, 1% NP40, 1% glycerol and 2 protease inhibitor tablets (Roche, Mannheim, Germany)) per plate was added to lyse the cells. The cells were scraped down and collected in appropriate 1.5 ml microcentrifuge tubes on ice, which were then vortexed once every 10 min 3 times and centrifuged for 20 min at 12,000 rpm 4 °C. The supernatants were transferred to another set of microcentrifuge tubes. These were the total protein samples. Lowry assay was used to determine protein concentrations in different solutions.

30 μg of each protein sample and protein marker were loaded to appropriate wells in the 10% stacking gels in presence of running buffer in a protein electrophoresis system. The running process occurred in 12% separating gels and took 150 min at 75 V, 400 amps, powered by a power supply. Then proteins were transferred to PVDF membranes (Immobilon transfer membranes, Millipore, USA) for 3 h at 85 V, 400 amps. Nonspecific protein binding was blocked in blocking buffer (5% milk in 1× TBS) for 1 h at room temperature. 1× TBS was used to wash off with blocking buffer and the PVDF membranes were rocked in 1:1000 primary (1°) antibody (Ab) solutions for at least 1 overnight. Then the 1° Ab TBS solutions were recycled. The PVDF membranes were washed with 1× TBS 3 times and soaked and rocked in 1:1000 secondary (2°) Ab solutions for 1 h at room temperature. The following antibodies were used: anti-Bad (Santa Cruz Biotechnology, CA, USA), anti-phospho-Bad^{Ser136} (Cell Signaling, Danvers, MA, USA), anti-Bcl-2 (BD, Pharmingen, San Jose, CA, USA), anti-calcineurin (BD, Pharmingen, San Jose, CA, USA), anti-caspase 3 (Santa Cruz Biotechnology, CA, USA), anti-caspase 9 (Santa Cruz Biotechnology, CA, USA), anti-cytochrome c (Santa Cruz Biotechnology, CA, USA), anti-Gαq/11 (Santa Cruz Biotechnology, CA, USA), anti-IGFIIR (Santa-Cruz Biotechnology, CA, USA), anti-PLC-β3 (Cell Signaling, Danvers, MA, USA), anti-phosoho-PLC-$β3^{Ser537}$ (Cell Signaling Danvers, MA, USA), anti-α-Tubulin (Santa Cruz Biotechnology, CA, USA), anti-goat-HRP (Santa Cruz Biotechnology, CA, USA), anti-rabbit-HRP (Santa Cruz Biotechnology, CA, USA) and anti-mouse-HRP (Santa Cruz Biotechnology, CA, USA).

The PVDF membranes were washed with 1× TBS 3 times and protein expressions were detected with Western blotting luminol reagent (PIERCE, Rockford, IL, USA). Restore western blot stripping buffer (Santa Cruz Biotechnology, CA, USA) was used to stripe off any Ab on the PVDF membranes and the membranes washed with DDW 2 to 3 times to any residue of the buffer.

2.6. JC-1 staining assay

H9c2 cardiomyoblasts were grown in a 12-well plate (1×10^5 cells/well) containing DMEM (10% CCS). Twenty-four hours later, the cells were deprived of serum for 4 h, and then 20, 40, 60, 80 and 100 μg/ml *C. pilosula* were added to appropriate wells followed by 10 μl 10^{-7} M AngII 1 h later, followed by 10^{-8} M Leu^{27}-IGFII after further 2 h. The cells were incubated in humidified air with 5% CO_2 at 37 °C. Twenty-four hours after administration of Leu^{27}-IGFII, 25 μl 200X JC-1 (5,5′,6,6′-tetrachloro-1,1′,3,3′-tetraethylbenzimidazolo carbocyanine iodide) stock solution (T-4069-1MG; Sigma, MO, USA) (1 mg/ml) was mixed with 4 ml de-ionised distiled water (DDW) and 1 ml 5× JC-1 staining buffer (Sigma, MO, USA) in the absence of light to make JC-1 staining mixture. 0.5 ml JC-1 staining mixture per well was added and then the plate was covered with tin foil and placed in humidified air (5% CO_2) for 20 min at 37 °C. During incubation, 5× JC-1 staining buffer was mixed with DDW in 1:4 ratio (=washing buffer). Each well was washed with 0.5 ml washing buffer 3 times after the 20-min incubation period. Finally 3 ml DMEM (10% CCS) was added to each well and then observe cells under fluorescent microscope using Cy3 (red) and FITC (green).

2.7. Co-immunoprecipitation (co-IP) of IGFIIR and Gαq association

H9c2 cells were grown in 10 cm culture dishes containing DMEM (10% CCS) to 80–90% confluency. Twenty-four hours later, the cells were deprived of serum for 4 h, and then 20, 40, and 60 μg/ml *C. pilosula* were added to appropriate dishes followed by 10^{-7} M AngII 1 h later, and then 10^{-8} M Leu^{27}-IGFII after further 2 h. The cells were incubated in humidified air (5% CO_2) for 24 h at 37 °C. Twenty-four hours after administration of Leu^{27}-IGFII, each plate was washed with 3 ml PBS twice and the remaining fluid in each plate was sucked off. Then 100 μl cell lysis buffer (for co-IP) (1.5 mM $MgCl_2$, 1% Triton X-100, 50 mM pH7.6 HEPES, 1 mM EDTA, 150 mM NaCl, 10% glycerol, 1 mM $NaVO_3$, 10 mM NaF, 10 mM β-glycerolphosphate, 5 protease inhibitor tablets and 50 ml DDW) per plate was added to lyse the cells, which were then scarped down and stored at -80 °C overnight. The method of obtaining total protein samples and protein quantification were the same as in Western blotting.

500 μl co-IP buffer ((1.5 mM $MgCl_2$, 1% Triton X-100, 50 mM pH7.6 HEPES, 1 mM EDTA, 150 mM NaCl, 10% glycerol, 1 mM $NaVO_3$, 10 mM NaF, 10 mM β-glycerolphosphate, and 500 ml DDW) was mixed with 5 μl protein G-agarose (Santa Cruz Biotechnology, CA, USA) and 100 μg protein sample in each 1.5 ml microcentrifuge tube. Nonspecific protein binding was blocked in blocking buffer for 1 h at room temperature. The methods for antibody binding and visualising protein expression were the same in western blot. The following Abs were used in this experiment: anti-Gαq/11 (Santa Cruz Biotechnology, CA, USA), anti-IGFIIR (Santa-Cruz Biotechnology, CA, USA) and anti-α-Tubulin (Santa Cruz Biotechnology, CA, USA), and Anti-Rabbit-HRP (Santa-Cruz Biotechnology, CA, USA).

2.8. Statistical analysis

Each sample was analysed based on results that were repeated at least three times and SigmaPlot 10.0 software and standard *t*-test was used to analyse each numeric data. In all cases, differences at $p < 0.05$ were regarded as statistically significant, ones at $p < 0.01$ or $p < 0.001$ were considered higher statistical significances.

3. Results

3.1. AngII enhanced the IGFIIR promoter activity and Dung-shen reversed this situation

To screen which traditional Chinese medical herb that down-regulate IGFII promoter activity that was elevated by AngII, Dr.

Chu cloned full-length IGFII promoter (P1) sequence and ligated that to luciferase reporter gene. 4 plasmids were constructed: CMV (positive control), Null (empty vector), P1 (full-length IGF2R promoter), and PGL_2. In the Dung-shen result, AngII along caused a 2.09-fold increase in IGFIIR activity (Fig. 1). The addition of *C. pilosula* showed 2.67-fold, 4.66-fold and 10.08-fold decrease at 1, 5 and 50 unit/μl, respectively. These results indicated that *C. pilosula* was able to regulate IGFIIR promoter activity that was highly elevated by AngII. So far 61 different traditional Chinese medical (TCM) herbs were already tested and categorised according to their effective doses; *C. pilosula* was one of the TCMs that downregulated IGFIIR promoter activity at low (1 unit/μl), medium (5 unit/μl) and high (50 unit/μl) doses. Therefore, it was selected for later experiments.

3.2. *C. pilosula attenuated AngII plus Leu^{27}-IGFII-induced the increase in cytosolic Ca^{2+} concentration*

In control, the cytosolic Ca^{2+} concentration was maintained in a basal level (top left corner, Fig. 2). AngII plus Leu^{27}-IGFII along caused a significant increase in cytosolic calcium, as indicated by increase in FITC intensity (centre upper panel, Fig. 2). The FITC signal was attenuated by *C. pilosula* in dose-dependent manner (top right corner and lower panel, Fig. 2). These results showed that AngII plus Leu^{27}-IGFII resulted in increase in cytosolic calcium concentration and this elevation of intracellular calcium was downregulated by *C. pilosula*. The results also indicated an increased PLC-β3 activity due to AngII plus Leu^{27}-IGFII, which was decreased by *C. pilosula*.

3.3. *AngII plus Leu^{27}-IGFII-induced calcium influx and apoptosis are downregulated by C. pilosula in H9c2 cells*

From previous results, *C. pilosula* reversed AngII plus Leu^{27}-IGFII-induced increase in intracellular Ca^{2+} concentration in H9c2 cells. However, how does *C. pilosula* affect intracellular Ca^{2+} concentration and apoptosis in the presence of AngII plus Leu^{27}-IGFII? Western blot analysis was conducted to investigate downregulating effect of *C. pilosula* on AngII plus Leu^{27}-IGFII-induced IGFII/IGFIIR pathway. Fig. 3(A) shows that activities of IGFIIR, Gαq, PLC-β3, p-PLC-β3^{Ser537} and calcineurin were significantly induced by 10^{-7} M AngII plus 10^{-8} M Leu^{27}-IGFII, in which IGFIIR, PLC-β, p-PLC-β3 and calcineurin displayed 40.62-fold, 1.18-fold, 177.93-fold and 9.32-fold increase compared to control, respectively (Fig. 3(B)). In contrast, *C. pilosula* decreased their levels in dose-dependent manner: IGFIIR (39.66%, 82.2% and 97.93% decrease by 20, 40 and 60 μg/ml *C. pilosula* compared to AngII + Leu^{27}-IGFII, respectively), PLC-β3 (24.79%, 56.3% and 65.73% decrease by 20, 40 and 60 μg/ml *C. pilosula* compared to AngII + Leu^{27}-IGFII, respectively), p-PLC-β3^{Ser537} (41.3%, 89.65% and 96.29% decrease by 20, 40 and 60 μg/ml *C. pilosula* compared to AngII + Leu^{27}-IGFII, respectively) and calcineurin (29.14%, 62.45% and 85.04% decrease by 20, 40 and 60 μg/ml *C. pilosula* compared to AngII + Leu^{27}-IGFII, respectively). In addition, AngII plus Leu^{27}-IGFII also significantly increased p-PLC-β3/PLC-β3 ratio (151.2-fold increase compared to control). However, *C. pilosula* decreased such ratio: 21.95%, 66.96% and 54.33% decrease by 20, 40 and 60 μg/ml *C. pilosula* compared to AngII + Leu^{27}-IGFII, respectively. These results indicated that *C. pilosula* is able to downregulate upstream factors of IGFII/IGFIIR pathway in a dose-dependent manner.

Increased calcineurin activity caused dephosphorylation and subsequent insertion into mitochondrial membranes of Bad. Then mitochondrial proteins, such as Apaf-1 and cytochrome *c* (Cyto *c*), were released. Again this event was induced by 10^{-7} M AngII plus 10^{-8} M Leu^{27}-IGFII along, in which unphosphorylated Bad and Cyto *c* increased by 9.68-fold and 9.96-fold compared to control (Fig. 3(C)), respectively. In contrast, *C. pilosula* decreased their levels in a dose-dependent manner: unphosphorylated Bad (9.3%, 67.96% and 94.94% decrease by 20, 40 and 60 μg/ml *C. pilosula* compared to AngII + Leu^{27}-IGFII, respectively) and Cyto *c* (10.9%, 67.83% and 95.09% decrease by 20, 40 and 60 μg/ml *C. pilosula* compared to AngII + Leu^{27}-IGFII, respectively) (Fig. 3(D)). However,

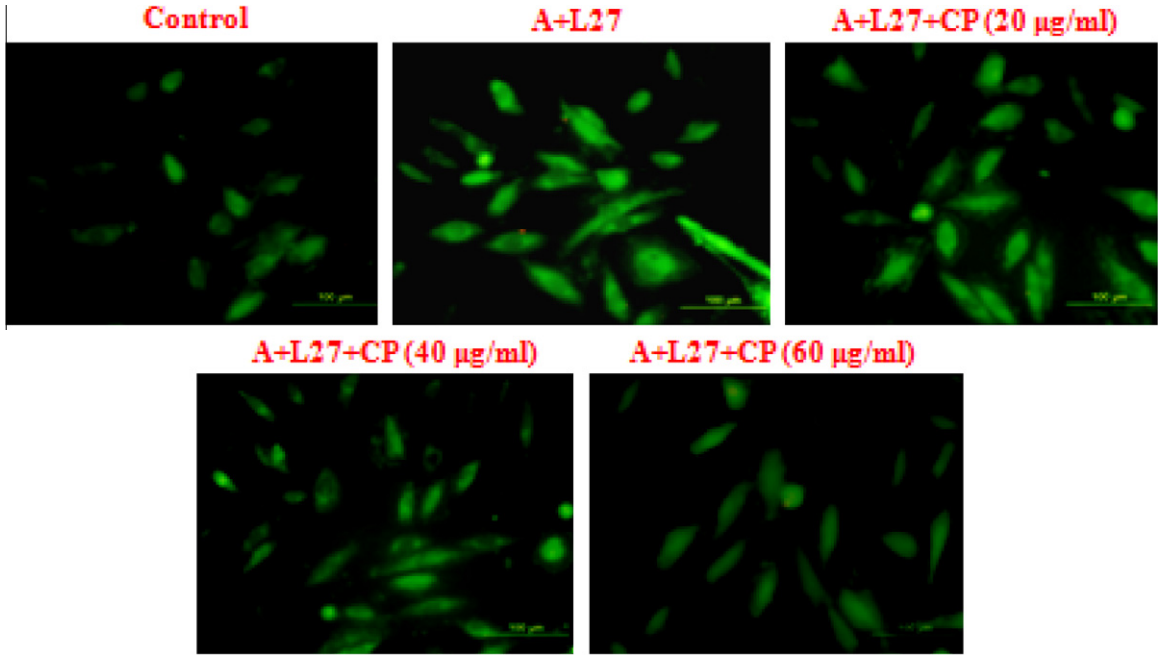

Fig. 2. *C. pilosula* attenuated AngII plus Leu^{27}-IGFII-induced Ca^{2+} influx. Twenty-four hours after growing H9c2 cells in 12-well plates, serum was derived for 4 h. *C. pilosula* was added first, followed by 10^{-7} M AngII after 1 h and then 10^{-8} M Leu^{27}-IGFII after another 2 h. Fluo 4-AM assay was conducted 24 h after addition of Leu^{27}-IGFII. Fluo 4-AM was used to dye cytosolic Ca^{2+} ions in H9c2 cells. A, AngII; concentration, 10^{-7} M; L27, Leu^{27}-IGFII; concentration, 10^{-8} M; CP, *C. pilosula*.

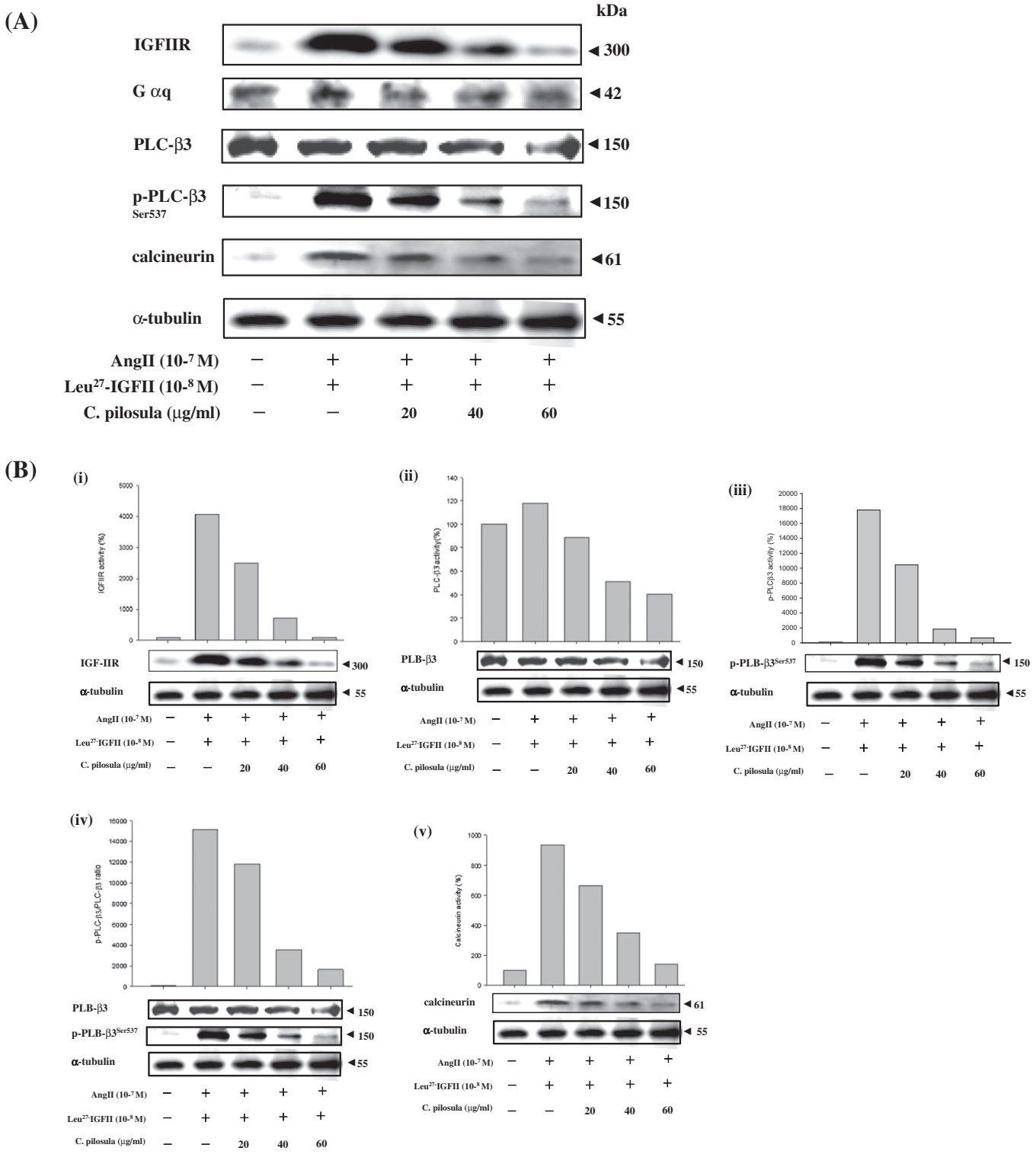

Fig. 3. *C. pilosula* inhibited IGFII/IGFIIR signaling pathway induced by AngII plus Leu^{27}-IGFII of H9c2 cardiomyoblast cells. Twenty-four hours after growing H9c2 cells in 10 cm plates, serum was derived for 4 h. *C. pilosula* was added first, followed by 10^{-7} M AngII after 1 h and then 10^{-8} M Leu^{27}-IGFII after another 2 h. Western blotting assay was conducted 24 h after addition of Leu^{27}-IGFII. (A) *C. pilosula* suppressed the protein levels of IGFII/IGFIIR signaling molecules, Gαq, PLC-β3, p-PLC-β3 and calcineurin by AngII plus Leu^{27}-IGFII. (B) Quantifications of IGFIIR, PLC-β3, p-PLC-β3 and calcineurin levels (n = 1). (C) *C. pilosula* inhibited the caspase 3 activity by AngII plus Leu^{27}-IGFII. (E) *C. pilosula* attenuated AngII plus Leu^{27}-IGFII-induced mitochondrial outer-membrane permeability. Twenty-four hours after growing H9c2 cells in 12-well plates, serum was derived for 4 h. *C. pilosula* was added first, followed by 10^{-7} M AngII after 1 h and then 10^{-8} M Leu^{27}-IGFII after another 2 h. Mitochondria (JC-1) staining assay was conducted 24 h after addition of Leu^{27}-IGFII. JC-1, or 5,5′,6,6′-tetrachloro-1,1′,3,3′-tetraethylbenzimidazolyl-carbocyanine iodide, was used to dye mitochondria.

p-Bad^{Ser136} and Bcl-2 were decreased by AngII plus Leu^{27}-IGFII but were increased by *C. pilosula* in a dose-dependent manner. These results indicated that *C. pilosula* was able to retain Bad in the cytosol to attenuate AngII plus Leu^{27}-IGFII-induced MOMP and the subsequent release of mitochondrial proteins in a dose-dependent manner.

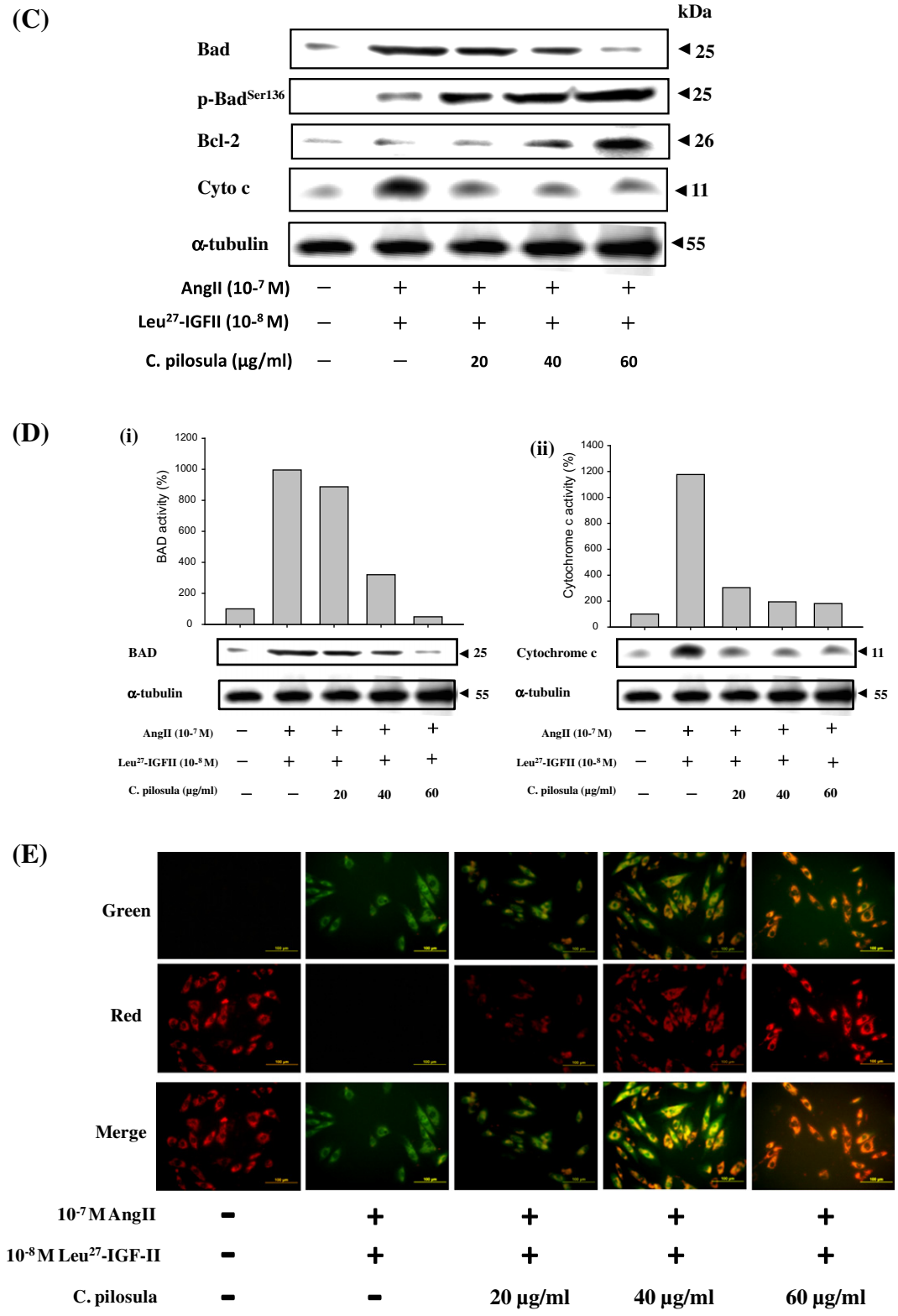

Fig. 3. (*continued*)

3.4. C. pilosula was able to lessen AngII plus Leu^{27}-IGFII-induced mitochondrial outer-membrane permeability (MOMP)

Binding of IGFII to IGFIIR leads to activation of PLC-β3 via Gαq. Subsequently, PLC-β3 activation leads to Ca^{2+} influx, calcineurin activation, and Bad insertion into mitochondrial membranes and MOMP (Chen et al., 2009). To observe the effect of *C. pilosula* on AngII plus Leu^{27}-IGFII-induced MOMP, JC-1 staining was conducted. When mitochondrial electron transport chain functions normally, JC-1 dye is in the form of J-aggregate, which emits at 530 nm and can visualised at Cy3 (red) (Cossarizza, Baccarani-Contri, Kalashnikova, & Franceschi, 1993; Reers, Smith, & Chen, 1991; Smi-

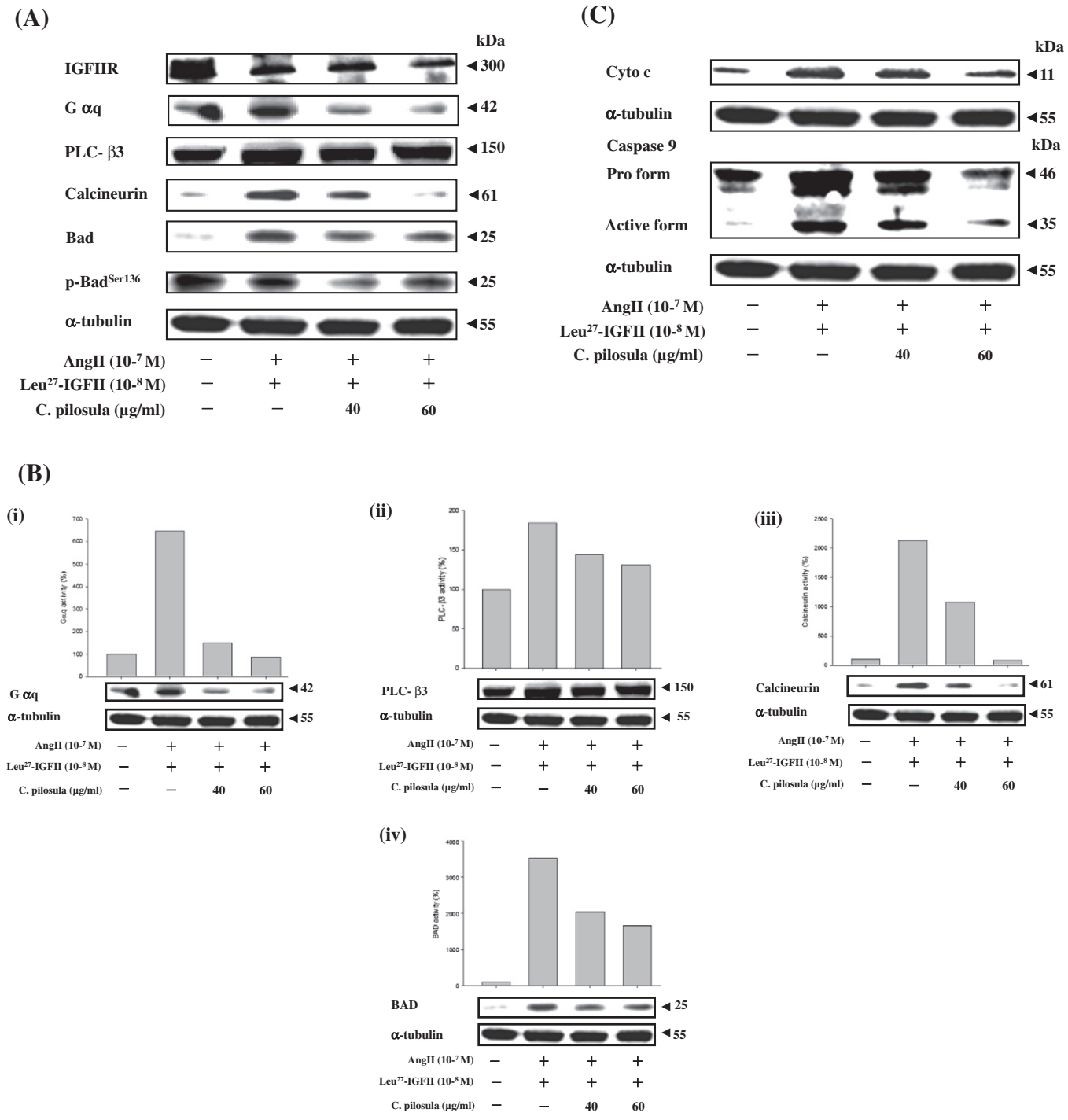

Fig. 4. *C. pilosula* was also able to suppress the IGFIIR apoptotic pathway in neonatal rat cardiomyocytes. Twenty-four hours after culturing neonatal rat cardiomyocytes in 10 cm plates, serum was derived for 4 h. *C. pilosula* was added first, followed by 10^{-7} M AngII after 1 h and then 10^{-8} M Leu^{27}-IGFII after another 2 h. Western blot was conducted 24 h after addition of Leu^{27}-IGFII. (A) Regulation of activity of IGFIIR, Gαq, PLCβ3, calcineurin, Bad and p-Bad^{Ser16} by AngII plus Leu^{27}-IGFII and *C. pilosula*. (B) Quantifications of Gαq, PLCβ3, calcineurin, and Bad levels ($n = 1$). (C) Regulation of activity of Cyto *c*, caspase 3, and caspase 9 by AngII plus Leu^{27}-IGFII and *C. pilosula*. (D) Quantifications of Cyto *c*, caspase 3, and caspase 9 levels ($n = 1$).

ley et al., 1991). When ETC. functions abnormally, mitochondrial membrane potential becomes unstable and JC-1 appears as JC-1 monomer, which emits at 530 nm and can be detected at FITC (green). This indicates an event of MOMP in a cell. Changes in Cy3 and FITC emission intensities can be used to detect changes of mitochondrial membrane potential and therefore changes of cellular metabolic state.

In control (i.e. no drug treatment), there were only strong Cy3 signals and no FITC (Fig. 3(E)). A very strong FITC signal was detected when 10^{-7} M AngII and 10^{-8} M Leu^{27}-IGFII were added along. Administration of 20, 40 and 60 μg/ml *C. pilosula* caused a weakening of FITC signals and increasing Cy3 signals. These results indicated that AngII plus Leu^{27}-IGFII along causes MOMP in H9c2 cardiomyoblasts and *C. pilosula* is able to reverse such mitochondrial membrane potential instability in a dose-dependent manner and the 60 μg/ml dose seems to be most effective.

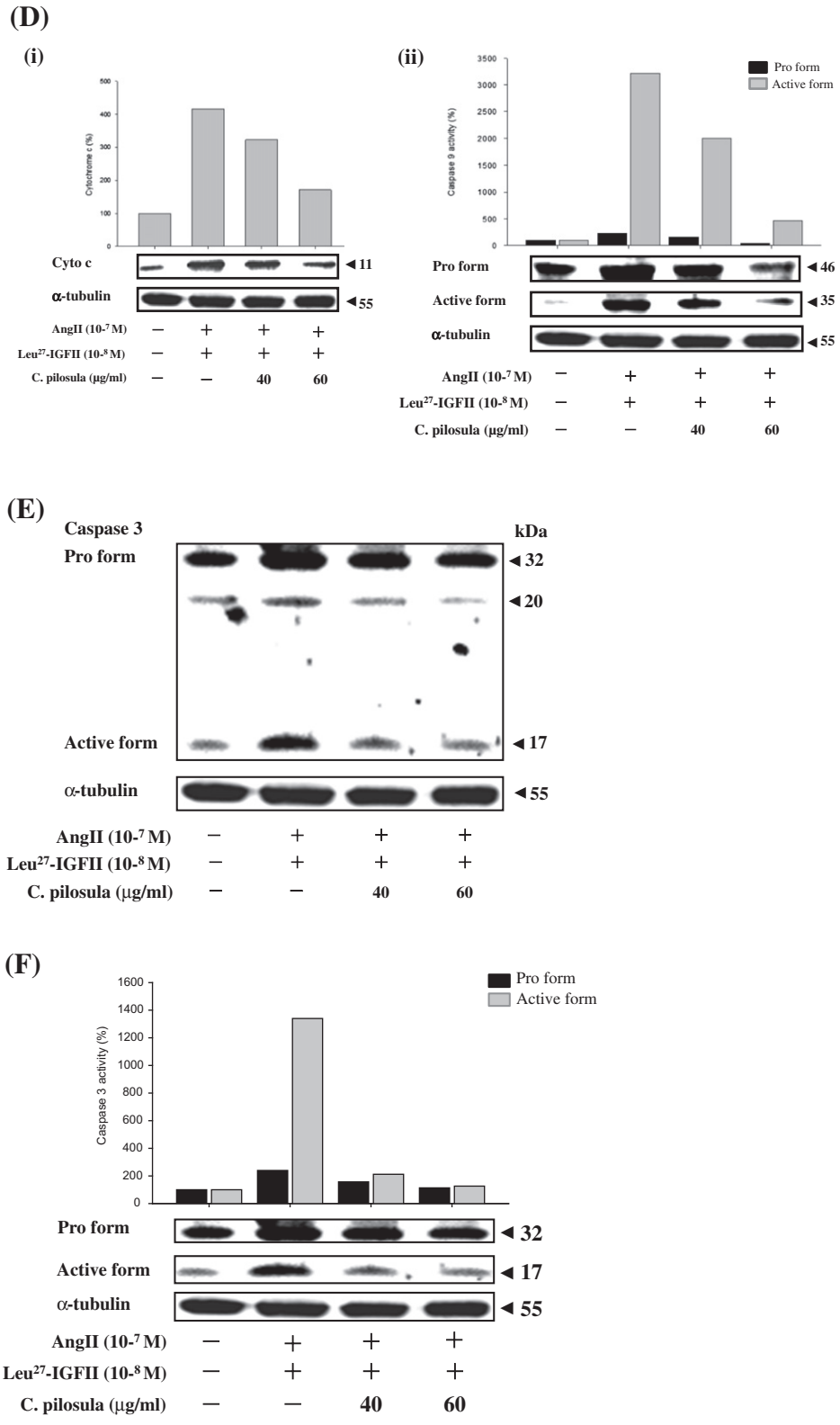

Fig. 4. (*continued*)

3.5. AngII plus Leu^{27}-IGFII-induced calcium influx and apoptosis are also downregulated by C. pilosula in neonatal rat primary cardiomyocytes

Neonatal primary cardiomyocytes from SD rats were grown in 10 cm culture plates and were deprived off serum for 4 h. 20, 40, and 60 μg/ml *C. pilosula* were added to appropriate dishes followed by 10^{-7} M AngII 1 h later, followed by 10^{-8} M Leu^{27}-IGFII after further 2 h. After 24 h, western blotting assay was conducted to confirm the western blot results in H9c2 cells that *C. pilosula* is able to suppress IGFIIR apoptotic pathway.

AngII plus Leu^{27}-IGFII significantly induced protein levels of IGFIIR, Gαq, PLC-β3, calcineurin and Bad (Fig. 4(A)), in which Gαq, PLC-β3, calcineurin and Bad showed 6.46-fold, 1.84-fold,

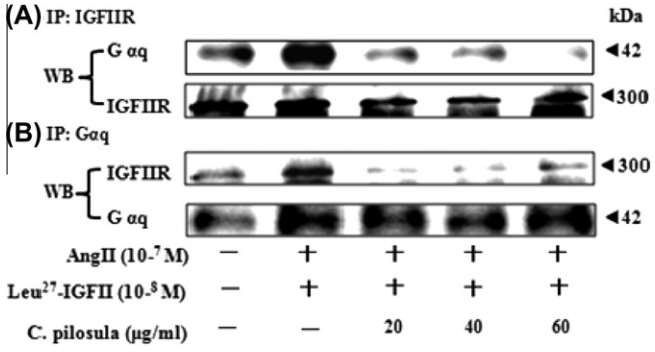

Fig. 5. *C. pilosula* attenuated AngII plus Leu^{27}-IGFII-induced IGFIIR-Gαq association in H9c2 cells. (A) Immunoprecipitated IGFIIR and then increased the Gαq and IGFIIR protein levels by western blotting. (B) Immunoprecipitated IGFIIR and then increased the IGFIIR and Gαq protein levels by western blotting.

21.32-fold and 35.15-fold increase compared to control, respectively. The following protein levels were downregulated by *C. pilosula* in a dose-dependent manner (Fig. 4(B)): Gαq (76.63% and 86.81% decrease by 40 and 60 μg/ml *C. pilosula* compared to AngII + Leu^{27}-IGFII, respectively), PLC-β3 (21.72% and 28.91% decrease by 40 and 60 μg/ml *C. pilosula* compared to AngII + Leu^{27}-IGFII, respectively), calcineurin (49.46% and 92.06% decrease by 40 and 60 μg/ml *C. pilosula* compared to AngII + Leu^{27}-IGFII, respectively), and Bad (42.01% and 52.71% decrease by 40 and 60 μg/ml *C. pilosula* compared to AngII + Leu^{27}-IGFII, respectively). Therefore, *C. pilosula* inhibited downstream factors of the IGFIIR pathway in neonatal rat cardiomyocytes. In contrast, p-Bad^{Ser136} was initially decreased by AngII plus Leu^{27}-IGFII, and then raised by *C. pilosula*.

AngII plus Leu^{27}-IGFII also significantly upregulated Cyto *c* and active form of caspase 9 in neonatal primary cardiomyocytes (4.16-fold and 32.1-fold compared to control, respectively) (Fig. 4(C) and (D)). However, *C. pilosula* also suppressed their levels: cytochrome *c* (22.47% and 58.79% decreased by 40 and 60 μg/ml *C. pilosula* compared to AngII + Leu^{27}-IGFII, respectively) and active caspase 9 (37.97% and 85.53% decreased by 40 and 60 μg/ml *C. pilosula* compared to AngII + Leu^{27}-IGFII, respectively).

Active caspase 3 was induced by AngII plus Leu^{27}-IGFII at 13.4-fold (Fig. 4(C) and (E)). This was again attenuated by *C. pilosula* dose-dependently (84.16% and 90.58% decreased by 40 and 60 μg/ml *C. pilosula* compared to AngII + Leu^{27}-IGFII, respectively).

Taken together, *C. pilosula* was capable of downregulating AngII plus Leu^{27}-IGFII-induced IGFIIR apoptotic pathway in primary neonatal cardiomyocytes as well.

3.6. *C. pilosula attenuated AngII plus Leu^{27}-IGFII-induced IGFII-Gαq interaction*

C. pilosula was previously shown to decrease activity of IGFIIR and Gαq and that of their downstream factors (Figs. 3 and 4(A) and (B)). Next, we investigated strength of the association between IGFIIR and Gαq. Because IGFIIR is a G protein-coupled receptor, it must associate with Gq protein first in order to relay an extracellular signal into H9c2 cells. Here, IGFIIR acts as a guanine nucleotide exchange factor that exchanges Gαq-bound GDP with GTP for Gq activation. Then Gαq dissociates from β and γ subunits and activates PLC-β3 (Chu et al., 2008).

AngII plus Leu^{27}-IGFII along increased IGFIIR-Gαq association significantly (Fig. 5). However, strength of this association was attenuated by *C. pilosula*. This proves that *C. pilosula* is able to downregulate IGFII/IGFIIR apoptotic pathway.

4. Discussion

Dr. Chu previously discovered that AngII or abdominal aortic ligation was able to induce expression of IGFII and IGFIIR and that IGFII is capable of binding to IGFIR and IGFIIR in order to cause cardiac hypertrophy (Chu et al., 2008). In earlier findings, binding of IGFI to IGFIR induces pathological cardiac hypertrophy (Miyashita, Takeishi, Takahashi, Kato, Kubota, & Tomoike, 2001). In addition, binding of IGFI to IGFIR or IGFIIR both induces physiological hypertrophy, in which when demand for higher blood flow is removed, cardiomyocytes return to non-hypertrophied size (Colan, 1997). However, binding of IGFII to IGFIIR induces pathological hypertrophy, in which there is an accumulation of intracellular Ca^{2+} ions and an increased activity of calcineurin (Lee et al., 2006). However, the elevated Ca^{2+} concentration and calcineurin activity lead to mitochondrial membrane potential instability and apoptosis of cardiomyocytes (Chu et al., 2008; Lee et al., 2006). Besides, Leu^{27}-IGFII, an analogue of IGFII (Sakano et al., 1991), strongly binds to IGFIIR and induces cardiomyocytes apoptosis *via* Gαq (Chen et al., 2009). Therefore, it was used here to enhance the apoptotic effect of AngII.

In this study, AngII plus Leu^{27}-IGFII was able to increase the amount of cytosolic Ca^{2+} ions in H9c2 cells (Fig. 2). However, this situation was reversed dose-dependently by *C. pilosula*, reducing cytosolic Ca^{2+} concentration similar to control. These indicated an elevation of PLC-β3 and calcineurin activity due to AngII plus Leu^{27}-IGFII and that *C. pilosula* was able lower PLC-β3 activity and the subsequent Ca^{2+} influx. In addition, calcineurin activity was increased by 9.32-fold (Fig. 3(B)(v)), and this was caused by a significant increase in PLC-β3 and p-PLC-β3 protein levels (Fig. 3(A) and (B)(ii, iii)), p-PLC-β3-to-PLC-β3 ratio (Fig. 3(B)(iv)), and cytosolic Ca^{2+} level (Fig. 2), since calcineurin activity is proportional to PLC-β3 activity and intracellular Ca^{2+} concentration (Lee et al., 2006). Moreover, Gαq, PLC-β3 and calcineurin were also elevated by AngII plus Leu^{27}-IGFII by 6.46-, 1.84-, and 21.32-fold, respectively, in neonatal SD rat primary cardiomyocytes (Fig. 4(B)(i, ii, iii)).

Then, there was a significant increase in unphosphorylated Bad (this was due to Ca^{2+} influx and increased calcineurin activity) and Cyto *c* and a decrease in p-Bad^{Ser136} (Fig. 3(C) and (D)). At increasing doses of *C. pilosula*, the amounts of unphosphorylated Bad and Cyto *c* displayed a decreasing trend. As a result, caspase 3 activity was also increased by AngII plus Leu^{27}-IGFII and downregulated by *C. pilosula* in a dosed-dependent manner. In addition, in neonatal SD rat primary cardiomyocytes, unphosphorylated Bad, Cyto *c*, caspase 9 and caspase 3 were significantly increased by AngII plus Leu^{27}-IGFII; and *C. pilosula* again dose-dependently reversed this situation (Fig. 4(A) and (B) (iv), 4(C) and 4(D)). Therefore, AngII plus Leu^{27}-IGFII is able to initiate an intrinsic, mitochondria-dependent apoptotic pathway via increase in Ca^{2+} influx and mitochondrial membrane potential instability in cardiomyocytes, where IGFIIR serves as a death receptor and IGFII/Leu^{27}-IGFII serves as a death ligand. This fits the model that was previously established in our lab, in which aorta abdominal ligation or pressure overload increases circulating AngII, production of IGFII/IGFIIR, Ca^{2+} influx, Ca^{2+} aggregation-induced MOMP and finally apoptosis (Chu et al., 2008; Lee et al., 2006). Finally, *C. pilosula* was able to suppress IGFII/IGFIIR apoptotic pathway by reducing Ca^{2+} influx and mitochondrial membrane potential instability.

Next, since AngII plus Leu^{27}-IGFII induced H9c2 apoptosis, it was reasonable to determine the level and the mechanism of AngII plus Leu^{27}-IGFII-induced apoptosis and the downregulating effect of this event by *C. pilosula*. This reduction of AngII plus Leu^{27}-IGFII-induced H9c2 apoptosis was again observed in downstream molecular markers in the IGFII/IGFIIR pathway, i.e. Bad, Cyto *c*,

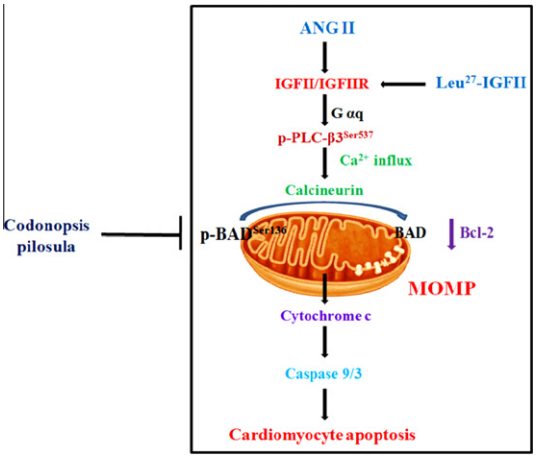

Fig. 6. AngII plus Leu^{27}-IGFII induces Ca^{2+} influx and apoptosis in myocardial cells. *C. pilosula* suppresses IGFIIR pathway by mediating through an inhibition of IGFIIR-Gαq upstream marker interaction.

caspase 9 and caspase 3 (Figs. 3(C), (E) and 4(C) and (D)), although there wasn't a clear trend in caspase 3 level. However, *C. pilosula* did result in reduction of caspase 3 activity in a dose-dependent manner, as seen in decreasing level of activated caspase 3 in neonatal SD rat primary cardiomyocytes (Fig. 4(C) and 4(D)(iii)). Collectively, because AngII plus Leu^{27}-IGFII induces Ca^{2+} influx and MOMP, which then result in apoptosis, and *C. pilosula* attenuates apoptosis induced by AngII plus Leu^{27}-IGFII, *C. pilosula* is able to suppress AngII plus Leu^{27}-IGFII-induced H9c2 apoptosis via reducing Ca^{2+} influx and MOMP.

Since *C. pilosula* is able to downregulate IGFII/IGFIIR apoptotic pathway, at which point on this pathway does *C. pilosula* mediate through? Since elevated level of unphosphorylated Bad by AngII plus Leu^{27}-IGFII was decreased by *C. pilosula*, it was reasonable to see whether *C. pilosula* would downregulate upstream factors in IGFII/IGFIIR pathway. AngII plus Leu^{27}-IGFII along caused significant increase in activity of these factors and p-PLC-β3/PLC-β3 ratio (Fig. 3(A) and (B)). In contrast, *C. pilosula* dose-dependently reduced levels of these upstream factors, including IGFIIR and p-PLC-β3/PLC-β3 ratio. The latter indicated that *C. pilosula* was able to suppress PLC-β3 phosphorylation in order to attenuate downstream Ca^{2+} influx and MOMP caused By AngII plus Leu^{27}-IGFII. Moreover, *C. pilosula* was able to downregulate AngII-induced IGFIIR promoter activity (Fig. 1); this is similar to IGFIIR levels observed in western blot results, where AngII plus Leu^{27}-IGFII induced significant increase in IGFIIR protein level (Fig. 6(A) and (B)(i)). These indicated that *C. pilosula* mediates through an upstream molecular marker. From Dr. Chu's studies, because activation of IGFII or IGFIIR genes requires both MEK and JNK, not p38, co-treatment with SB203580 should show results lower protein levels of IGFIIR, cytochrome *c* and active form of caspase 3 (Lee et al., 2006). Therefore, *C. pilosula* suppresses IGFII/IGFIIR apoptotic pathway by mediating through MEK, JNK, or other upstream molecular marker.

In addition, since *C. pilosula* downregulated AngII plus Leu^{27}-IGFII-induced IGFII/IGFIIR pathway, there must be an effect of *C. pilosula* on IGFIIR-Gαq interaction. IGFIIR-Gαq interaction was significantly upregulated by AngII plus Leu^{27}-IGFII; in contrast *C. pilosula* reduced this event, as indicated in Fig. 5. This indicated that *C. pilosula* suppresses IGFII/IGFIIR pathway by decreasing IGFIIR-Gαq. Subsequently, there is a downregulation of IGFII/IGFIIR downstream markers (such as PLC-β3, p-PLC-β3, unphosphorylated Bad and caspase 3) (Fig. 3), Ca^{2+} influx and MOMP.

In conclusion, in this study, it was found that AngII plus Leu^{27}-IGFII induced Ca^{2+} influx, MOMP and a significant increase in apoptosis in H9c2 cells and neonatal rat cardiomyocytes. However, *C. pilosula* reduced these events in a dose-dependent manner. Moreover *C. pilosula* was able reduced AngII plus Leu^{27}-IGFII-induced IGFIIR activity. Therefore, *C. pilosula* suppresses IGFII/IGFIIR pathway by mediating through an upstream marker.

Acknowledgment

This study is supported in part by Taiwan Department of Health Clinical Trial and Research Center of Excellence (DOH101-TD-B-111-004).

References

Atlas, S. A. (2007). The renin–angiotensin aldosterone system: Pathophysiological role and pharmacologic inhibition. *Journal of Managed Care Pharmacy, 13*(8), S9–S20.

Basso, N., & Terragno, N. A. (2001). History about the discovery of the renin–angiotensin system. *Hypertension, 38*(6), 1246–1249.

Brown, A. L., Graham, D. E., Nissley, S. D., Hill, D. J., Strain, A. J., & Rechler, M. M. (1986). Development regulation of insulin-like growth factor II mRNA in different rat tissues. *Journal of Molecular Endocrinology, 261*, 13144–13150.

Chen, R. J., Wu, H. C., Chang, M. H., Lai, C. H., Tien, Y. C., Hwang, J. M., et al. (2009). Leu27IGF2 plays an opposite role to IGF1 to induce H9c2 cardiomyoblast cell apoptosis via G q signaling. *Journal of Molecular Endocrinology, 43*(6), 221–230.

Chu, C. H., Tzang, B. S., Chen, L. M., Liu, C. J., Tsai, F. J., Tsai, C. H., et al. (2008). Activation of IGF2R induces mitochondrial-dependent apoptosis through Gq and downstream calcineurin signaling in myocardial cells. *Endocrinology, 150*(6), 2723–2731.

Colan, S. D. (1997). Mechanics of left ventricular systolic and diastolic function in physiologic hypertrophy of the athlete's heart. *Cardiology Clinics, 15*(3), 355–372.

Cossarizza, A., Baccarani-Contri, M., Kalashnikova, G., & Franceschi, C. (1993). New method for the cytofluorimetric analysis of mitochondrial membrane potential using the J-aggregate forming lipophilic cation 5,5′,6,6′-tetrachloro-1,1′,3,3′-tetraethylbenzimidazolcarbocyanine iodide (JC-1). *Biochemical and Biophysical Research Communications, 197*(1), 40–45.

Delafontaine, P., Song, Y. H., & Li, Y. (1995). Insulin-like growth factor I and its binding proteins in the cardiovascular system. *Cardiovascular Research, 30*, 825–834.

Engelmann, G. L., Boehm, K. D., Haskell, J. F., Khairallah, P. A., & Ilan, J. (1989). Insulin-like growth factors and neonatal cardiomyocyte development: Ventricular gene expression and membrane receptor variations in normotensive and hypertensive rats. *Molecular and Cellular Endocrinology, 63*(1–2), 1–14.

Ghosh, P., Dahms, N. M., & Kornfeld, S. (2003). Mannose 6-phosphate receptors: New twists in the tale. *Nature Reviews Molecular Cell Biology, 4*(3), 202–212.

Heineke, J., & Molkentin, J. D. (2006). Regulation of cardiac hypertrophy by intracellular signaling pathways. *Nature Reviews Molecular Cell Biology, 7*(8), 589–600.

Huang, C. Y., Hao, L. Y., & Buetow, D. E. (2002). Insulin-like growth factor-II induces hypertrophy of adult cardiomyocytes via two alternative pathways. *Cell Biology International, 26*(8), 737–739.

Humbel, R. E. (1990). Insulin-like growth factors I and II. *European Journal of Biochemistry, 190*(3), 445–462.

Kluge, A., Zimmermann, R., Munkel, B., Verdouw, P. D., Schaper, J., & Schaper, W. (1995). Insulin-like growth factor II is an experimental stress inducible gene in a porcine model of brief coronary occlusions. *Cardiovascular Research, 29*(5), 708–716.

Kuo, W. W., Liu, C. J., Chen, L. M., Wu, C. H., Chu, C. H., Liu, J. Y., et al. (2006). Cardiomyoblast apoptosis induced by insulin-like growth factor (IGF)-I resistance is IGF-II dependent and synergistically enhanced by angiotensin II. *Apoptosis, 11*(7), 1075–1089.

Laureys, G., Barton, D. E., Ullrich, A., & Francke, U. (1988). Chromosomal mapping of the gene for the type II insulin-like growth factor receptor/cation-independent mannose 6-phosphate receptor in man and mouse. *Genomics, 3*(3), 224–229.

Lee, S. D., Chu, C. H., Huang, E. J., Lu, M. C., Liu, J. Y., Liu, C. J., et al. (2006). Roles of insulin-like growth factor II in cardiomyoblasts apoptosis and in hypertensive rat heart with abdominal aorta ligation. *American Journal of Physiology – Endocrinology and Metabolism, 291*(2), E306–E314.

LeRoith, D., Werner, H., Beitner-Johnson, D., & Roberts, C. T. Jr., (1995). Molecular and cellular aspects of the insulin-like growth factor I receptor. *Endocrine Reviews, 16*(2), 143–163.

Matthews, K. G., Devlin, G. P., Conaglen, J. V., Stuar, S. P., Aitken, W. M., & Bass, J. J. (1999). Changes in IGFs in cardiac tissue following myocardial infarction. *Journal of Endocrinology, 163*(3), 433–445.

Miyashita, T., Takeishi, Y., Takahashi, H., Kato, S., Kubota, I., & Tomoike, H. (2001). Role of calcineurin in insulin-like growth factor-1-induced hypertrophy of cultured adult rat ventricular myocytes. *Japanese Circulation Journal, 65*(9), 815–819.

O'Dell, S. D., & Day, I. N. M. (1998). Molecules in focus: Insulin-like growth factor II (IGF-II). *The International Journal of Biochemistry & Cell Biology, 30*, 767–771.

Oshima, A., Nolan, C. M., Kyle, J. W., Grubb, J. H., & Sly, W. S. (1988). The human cation-independent mannose 6-phosphate receptor. Cloning and sequence of

the full-length cDNA and expression of functional receptor in COS cells. *Journal of Biological Chemistry, 263*(5), 2553–2562.

Park, G. H., & Buetow, D. E. (1991). Genes for insulin-like growth factors I and II are expressed in senescent rat tissues. *Gerontology, 37*(6), 310–316.

Reers, M., Smith, T. W., & Chen, L. B. (1991). J-aggregate formation of carbocyanine as a quantitative fluorescent indicator of membrane potential. *Biochemistry, 30*(18), 4480–4486.

Sakano, K., Enjoh, T., Numata, F., Fujiwara, H., Marumoto, Y., Higashihashi, N., et al. (1991). The design, expression, and characterisation of human insulin-like growth factor II (IGF-II) mutants specific for either the IGF-II/cation-independent mannose 6-phosphate receptor or IGF-I receptor. *Journal of Biological Chemistry, 266*(31), 20626–20635.

Sklar, M. M., Thomas, C. L., Municchi, G., Roberts, C. T., Jr., LeRoith, D., Kiess, W., et al. (1992). Developmental expression of rat insulin-like growth factor-II/mannose 6-phosphate receptor messenger ribonucleic acid. *Endocrinology, 130*(6), 3484–3491.

Smiley, S. T., Reer, M., Mottola-Hartshorn, C., Lin, M., Chen, A., Smith, T. W., Steele, G. D., Jr., Chen, L. B. (1991). Intracellular heterogeneity in mitochondrial membrane potentials revealed by a J-aggregate-forming lipophilic cation JC-1. *Proceedings of the National Academy of Sciences of the United States of America, 88*(9), 3671-3675.

Sun, F. L., Dean, W. L., Kelsey, G., Allen, N. D., & Relk, W. (1997). Transactivation of Igf2 in a mouse model of Beckwith–Wiedemann Syndrome. *Nature, 389*(6653), 809–815.

Tappy, L., Fujita-Yamaguchi, Y., LeBon, T. R., & Boden, G. (1988). Antibodies to insulin-like growth factor I receptors in diabetes and other disorders. *Diabetes, 37*, 1708–1714.

Tsuruzoe, K., Emkey, R., Kriauciunas, K. M., Ueki, K., & Kahn, C. R. (2001). Insulin receptor substrate 3 (IRS-3) and IRS-4 impair IRS-1- and IRS-2-mediated signaling. *Molecular and Cellular Biology, 21*(1), 26–38.

Wang, Z. T., Ng, T. B., Yeung, H. W., & Xu, G. J. (1996). Immunomodulatory effect of a polysaccharide-enriched preparation of *Codonopsis pilosula* roots. *General Pharmacology, 27*(8), 1347–1350.